Biochemistry

 Volume 38, Number 16 April 20, 1999

Accelerated Publications

Internal Dynamics of the Nicotinic Acetylcholine Receptor in Reconstituted Membranes†

John E. Baenziger,* Tim E. Darsaut, and Mary-Louise Morris

Department of Biochemistry, Microbiology, and Immunology, University of Ottawa, Ottawa, Ontario, Canada K1H 8M5

Received January 26, 1999; Revised Manuscript Received March 8, 1999

ABSTRACT: The structure and $^1H/^2H$ exchange kinetics of affinity-purified nAChR reconstituted into egg phosphatidylcholine membranes with increasing levels of either dioleoylphosphatidic acid (DOPA) or cholesterol (Chol) have been examined using infrared spectroscopy. All spectra of the reconstituted nAChR membranes recorded after 72 h in ^2H_2O exhibit comparable amide I band shapes, suggesting a similar secondary structure for the nAChR in each lipid environment. Increasing levels of either DOPA or Chol, however, lead to an increasing intensity of the amide II band, indicating a decreasing proportion of nAChR peptide hydrogens that have exchanged for deuterium. Spectra recorded as a function of time after exposure of the nAChR to ^2H_2O show that the presence of either lipid slows down the $^1H/^2H$ exchange of those peptide hydrogens that normally exchange on the minutes to hours time scale. The slowing of peptide $^1H/^2H$ exchange correlates with both an increasing ability of the nAChR to undergo agonist-induced conformational change [Baenziger, J. E., Morris, M.-L., Darsaut, T. E., and Ryan, S. E. (1999) in preparation] and possibly a decreasing membrane fluidity. Our data suggest that lipid composition dependent changes in nAChR peptide $^1H/^2H$ exchange kinetics reflect altered internal dynamics of the nAChR. Lipids may influence protein function by changing the internal dynamics of integral membrane proteins.

The nicotinic acetylcholine receptor (nAChR)[1] from *Torpedo* is a large neurotransmitter gated transmembrane ion channel that is used extensively as a model for studying lipid−protein interactions (*1*, *2*). The nAChR transiently gates open to cations in response to the binding of agonists, such as acetylcholine and carbamylcholine. Prolonged exposure to both agonists and a variety of noncompetitive antagonists leads to the formation of a channel inactive/desensitized state.

The ability of affinity-purified nAChR to conduct cations across the membrane and undergo the resting to desensitized conformational transition is highly sensitive to the composition of the surrounding lipid membrane. In pioneering studies, Fong and McNamee examined both the flux capabilities and the ligand binding properties of the nAChR reconstituted into membranes composed of a variety of different lipids and concluded that an optimal membrane fluidity as well as the presence of both cholesterol (Chol) and anionic lipids, such as dioleoylphosphatidic acid (DOPA), are required to support a functional nAChR (*3*). The specific lipid requirements were suggested to result from the binding of each lipid to distinct sites on the nAChR with the consequent formation of specific secondary structures (*4*−*7*).

† This work was supported by a grant from the Medical Research Council of Canada to J.E.B.

* To whom correspondence should be addressed.

[1] Abbreviations: Chol, cholesterol; DOPA, dioleoylphosphatidic acid; EPC, egg phosphatidylcholine; FTIR, Fourier transform infrared; nAChR, nicotinic acetylcholine receptor.

10.1021/bi990181l CCC: $18.00
Published on Web 04/02/1999

Subsequent studies, however, have provided a controversial picture of the mechanisms of lipid−protein interactions. Some physical studies have found no correlation between bulk fluidity and function in reconstituted nAChR membranes, suggesting a predominant role for specific lipid binding sites (*7*, *8*). In contrast, the ability of structurally diverse lipids to support nAChR function argues for a nonspecific mechanism of lipid−protein interactions (*8*, *9*). Recent Fourier transform infrared (FTIR) studies have also been unable to detect any of the changes in nAChR secondary structure reported previously in the presence of Chol and/or DOPA (*10*).

Our working hypothesis is that while specific lipid binding sites are likely important, membrane fluidity can influence the cation flux properties of the nAChR by modulating the natural equilibrium between the resting and desensitized states. To test this hypothesis, we reconstituted the nAChR into egg phosphatidylcholine (EPC) membranes with increasing levels of either DOPA or Chol, expecting that both lipids would individually decrease membrane fluidity and thus, according to our hypothesis, stabilize the nAChR in a functional resting conformation. In a separate report, we show that increasing levels of either lipid increasingly stabilize the nAChR in a conformation that is capable of undergoing agonist-induced conformational change (*11*). In the course of this study, we discovered that the nAChR peptide $^1H/^2H$ exchange kinetics are strongly influenced by lipid composition in a manner that might correlate with changes in membrane fluidity. The exchange experiments suggest that the amplitudes and/or rates of internal nAChR motions are influenced by lipid composition. Modulation of the dynamics of internal protein motions could serve as a general mechanism by which membranes influence integral membrane protein function.

EXPERIMENTAL PROCEDURES

Sample Preparation. The nAChR was affinity-purified on a bromoacetylcholine bromide derivatized Bio-Rad Affi-Gel 201 column (Richmond, CA) and then reconstituted into membranes composed of EPC with varying levels of either DOPA or Chol as described by McCarthy and Moore (*12*). EPC and DOPA were from Avanti Polar lipids, Inc. (Alabaster, AL). Cholesterol was from Sigma. Frozen *Torpedo californica* electric tissue was from Marinus (Long Beach, CA). In all cases except for the 9:1 molar ratios of EPC/DOPA and EPC/Chol, each reconstitution was performed between 2 and 5 times.

Transmission FTIR. A series of the reconstituted nAChR membranes (EPC with increasing levels of either DOPA or Chol) each containing 250 μg of nAChR protein in ^1H_2O buffer were centrifuged and the pellets resuspended in ^2H_2O/phosphate buffer 2 times. Each nAChR sample was left in ^2H_2O at 4 °C to exchange peptide N−^{1}H for N−^{2}H. After precisely 72 h in ^2H_2O, each was frozen in liquid nitrogen and stored at −80 °C. Samples were individually thawed prior to use, centrifuged, and resuspended in 30 μL of ^2H_2O buffer. Each nAChR solution was then deposited on a 1 cm diameter CaF_2 window and the excess buffer evaporated with a stream of dry nitrogen. The dried nAChR film was rehydrated with 8 μL of *Torpedo* Ringer buffer in ^2H_2O (250 mM NaCl, 5 mM KCl, 2 mM $MgCl_2$, 3 mM $CaCl_2$, and 5 mM Na_2HPO_4, pD 6.6) and sandwiched between a second CaF_2 window with a 12 μm Teflon spacer. Spectra were recorded at 22.5 °C using a thermostatically controlled transmission cell on either a Bio-Rad FTS 575C or a FTS 40 spectrometer, both equipped with a DTGS detector. Spectra were examined to remove trace water vapor absorbencies using GRAMS/32 software as described by Reid et al. (*13*; with $\gamma = 3$ and a smoothing of 0%). Deconvolution for visualization of the amide I component bands was performed using the method of Kauppinen et al. with $\gamma = 17.0$ and a resolution enhancement factor of 2.2 (*21*). Care was taken to ensure that all samples were exposed to ^2H_2O for equivalent lengths of time. In most cases, the stringent exchange conditions led to slightly reduced levels of peptide $^1H/^2H$ relative to those reported previously (*14*).

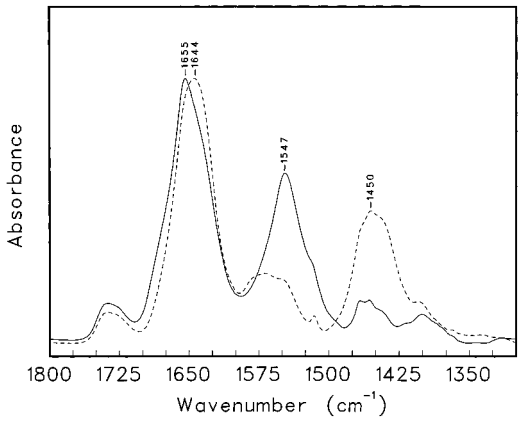

FIGURE 1: FTIR spectra of the nAChR recorded in both ^1H_2O (solid line) and ^2H_2O (dashed line) buffer. The spectrum of the nAChR in ^2H_2O was recorded after prior exposure of the nAChR to ^2H_2O buffer for 3 days at 4 °C. The absorbance of either ^1H_2O or ^2H_2O buffer has been subtracted from each spectrum.

Kinetics of Peptide Hydrogen/Deuterium Exchange. The peptide hydrogen/deuterium exchange kinetics were examined by recording spectra of the nAChR using the attenuated total reflectance technique. The nAChR in ^1H_2O was deposited on the surface of a germanium internal reflection element. The bulk aqueous solvent was evaporated with a gentle stream of N_2 gas and the film immediately rehydrated with *Torpedo* Ringer buffer in ^1H_2O. After the acquisition of one spectrum, the ^1H_2O buffer was removed from the attenuated total reflectance sample compartment and replaced with ^2H_2O buffer. Several spectra were recorded at 2 cm^{-1} resolution over the next 12 h with increasing numbers of scans, varying from 50 to 1500 scans per spectrum. All experiments were performed at 22.5 °C. Equivalent levels of ^2H_2O were subtracted from all spectra. The spectra were base-line-corrected between 1800 and 1300 cm^{-1} before measurement of the amide I and amide II band intensities. The presented amide II/amide I ratios differ slightly from those reported previously because of the applied base line correction (*10*).

RESULTS

nAChR Structure and Dynamics. FTIR spectra of the nAChR recorded in both ^1H_2O and ^2H_2O buffer exhibit a number of vibrational bands that are sensitive to the structure and dynamics of reconstituted nAChR membranes (Figure 1). The most intense feature in the spectra is the broad amide

I contour between 1600 and 1700 cm^{-1} which reflects predominantly the C═O stretching vibration of the polypeptide backbone. The amide I contour consists of a number of overlapping component bands each at a frequency characteristic of a specific type of secondary structure. The main α-helical and *β*-sheet vibrations are centered at frequencies between 1650 and 1660 cm^{-1} and between 1630 and 1640 cm^{-1}, respectively. Detailed analyses of the location and relative intensities of these and other amide I component bands have shown that the nAChR is a mixed α/*β* protein with a slight predominance of α-helical secondary structures (see ref *15* and references cited within).

Most amide I band analyses are performed using spectra acquired from proteins immersed in ^2H_2O buffer. While this eliminates complications that arise from the broad overlapping ^1H_2O vibration centered near 1640 cm^{-1}, the exchange of peptide N−^{1}H by N−^{2}H in ^2H_2O leads to subtle downshifts in the frequencies of a number of amide I component bands. The nAChR α-helical vibration shifts from near 1655 cm^{-1} in ^1H_2O down to between 1640 and 1650 cm^{-1} in ^2H_2O whereas the *β*-sheet vibration undergoes a much smaller downshift in frequency (*14*). Significantly, these and other band shifts lead to changes in the overall shape of the amide I contour (Figure 1). Previous studies have shown that roughly 60% of the nAChR peptide hydrogens exchange for deuterium over the first 12 h after exposure to ^2H_2O, leading to continual changes in shape of the amide I band over this time period (*14*). Even after 3 days exposure to ^2H_2O, subtle changes in amide I band shape are observed with time due to increasing levels of peptide $^1H/^2H$ exchange (*22*).

To accurately compare the secondary structures of the nAChR in EPC membranes with increasing levels of either DOPA or Chol, infrared spectra must be recorded under conditions that minimize experimental variations in the levels of peptide $^1H/^2H$ exchange. We simultaneously exposed all samples to ^2H_2O for precisely 72 h at 4 °C and then froze each sample at −80 °C. Samples were individually thawed and spectra recorded at 22.5 °C using a thermostatically controlled transmission cell (see Experimental Procedures for details). Resolution enhancement of the resulting spectra recorded from each of the reconstituted membranes reveal the expected amide I component bands [Figure 2, left panels in both (A) and (B)]. The two predominant bands centered near 1655 and 1635 cm^{-1} are characteristic of α-helix and *β*-sheet, respectively. The relative intensities of the various component bands are similar in all the spectra, indicating that the secondary structure of the nAChR is essentially lipid-independent. Increasing levels of either lipid, however, lead to a slight increase in intensity near 1655 cm^{-1} concomitant with a slight decrease in intensity between 1640 and 1650 cm^{-1} (the EPC/Chol 1:1 data are an exception and are discussed below). These subtle spectral changes are the opposite of those observed over the time course of peptide $^1H/^2H$ exchange and suggest that the presence of either DOPA or Chol in the reconstituted membranes leads to a reduction in the number of α-helical peptide hydrogens that have exchanged for deuterium after 3 days in ^2H_2O.

A reduced level of peptide $^1H/^2H$ exchange with increasing levels of either DOPA or Chol in the EPC membranes was confirmed by examining the residual intensity of the amide II vibrations in each spectrum. The amide II band reflects primarily peptide N−^{1}H bending and undergoes a shift in

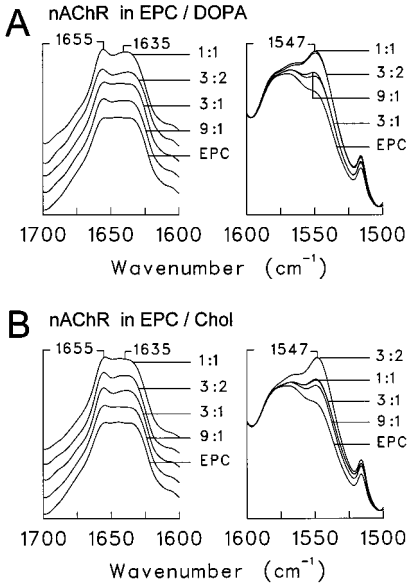

FIGURE 2: Deconvolved amide I band and residual amide II band intensity in FTIR spectra recorded from the nAChR reconstituted into EPC membranes with increasing levels of (A) DOPA and (B) Chol. The deconvolved amide I band for the nAChR in each lipid membrane is presented in the left panel of both (A) and (B). The amide II band in each nondeconvolved spectrum is presented in the right panel of both (A) and (B). Each spectrum is identified by the molar ratio of either EPC/DOPA (A) or EPC/Chol (B) in the reconstituted membrane. All samples were exposed to ^2H_2O buffer for 72 h at 4 °C prior to data acquisition. A spectrum of ^2H_2O buffer has been subtracted from each spectrum.

frequency from near 1547 cm^{-1} in ^1H_2O down to near 1450 cm^{-1} in ^2H_2O (Figure 1). As shown in the right panels of both Figure 2A and Figure 2B, increasing levels of either lipid generally lead to an increase in the residual amide II band intensity and thus a decrease in the levels of peptide $^1H/^2H$ exchange. For the nAChR in EPCmembranes, roughly 80% of the peptide hydrogens have exchanged for deuterium after 72 h in ^2H_2O. In contrast, roughly 65% of the peptide hydrogens have exchanged for deuterium with the nAChR reconstituted into either 3:2 EPC/DOPA or 3:2 EPC/Chol membranes (these values were calculated as described in ref *14*). Roughly 65% of the peptide hydrogens also exchange for deuterium under these exchange conditions for the nAChR in 3:1:1 EPC/DOPA/Chol membranes (data not shown). Significantly, the magnitudes of the differences in the levels of peptide $^1H/^2H$ exchange for the nAChR in the different lipid membranes are sufficient to account for the magnitudes of the observed changes in amide I band shape (data not shown; see ref *10* for details). This observation confirms that the above-noted changes in amide I band shape result from variations in the levels of peptide $^1H/^2H$ exchange as opposed to changes in nAChR secondary structure. The degrees of lipid-dependent variation in the relative levels of $^1H/^2H$ exchange are highly reproducible and are too large to be attributed to experimental variability in the exposure of samples to ^2H_2O. The noted spectral variations must therefore reflect *intrinsic* differences in the $^1H/^2H$ exchange kinetics of the nAChR in the different lipid membranes.

The effects of high levels of both DOPA and Chol on nAChR peptide $^1H/^2H$ exchange kinetics were examined further by recording FTIR spectra as a function of time after exposure of the nAChR to ^2H_2O buffer. Figure 3A compares

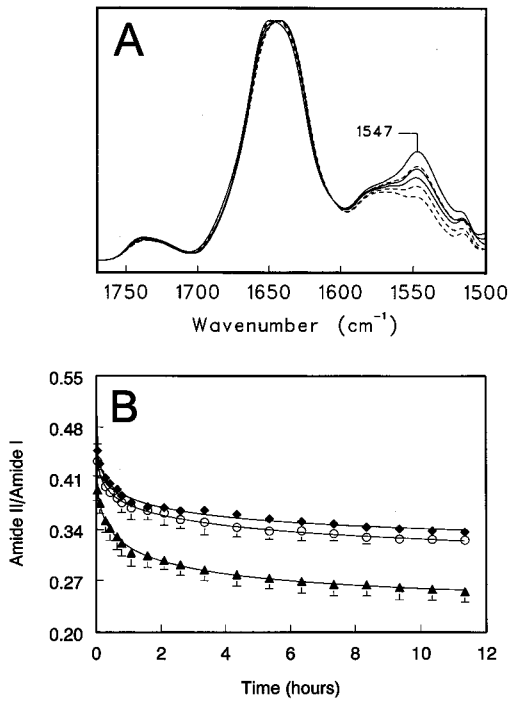

FIGURE 3: (A) FTIR spectra recorded over time after exposure of the nAChR in either 3:2 EPC/DOPA (solid line) or EPC alone (dashed line) membranes to ^2H_2O. Spectra were recorded from top to bottom after roughly 2 min, 2 h, and 10 h exposure to ^2H_2O. (B) Time course for the exchange of peptide hydrogens for deuterium as monitored by changes in the amide II/amide I band intensity ratio as a function of time after exposure of the nAChR in either 3:2 EPC/DOPA (solid diamonds), 3:2 EPC/Chol (open circles), or EPC alone (solid triangles) to ^2H_2O. Error bars depicting the standard deviation are presented when the standard deviation is larger than the size of the symbol. Each experiment was performed 3 times.

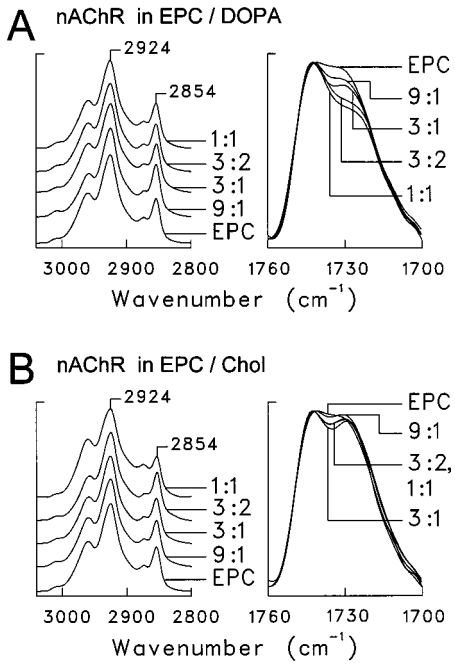

FIGURE 4: C−H stretching and carbonyl stretching regions in FTIR spectra recorded from the nAChR reconstituted into EPC membranes with increasing levels of (A) DOPA and (B) Chol. The C−H stretching region for the nAChR in each lipid membrane is presented in the left panel of both (A) and (B). The carbonyl stretching region in deconvolved spectra is presented in the right panel of both (A) and (B). Each spectrum is identified by the molar ratio of either EPC/DOPA (A) or EPC/Chol (B) in the reconstituted membrane. All samples were exposed to ^2H_2O buffer for 72 h at 4 °C prior to data acquisition. A spectrum of ^2H_2O buffer has been subtracted from each spectrum.

the residual amide II band intensities in spectra recorded from the nAChR in both EPC and 3:2 EPC/DOPA membranes at selected times over the first 12 h after exposure to ^2H_2O. Figure 3B summarizes the time dependence of exchange, as measured by changes in amide II/amide I band intensity. The data clearly show that the exchange kinetics for the nAChR in both 3:2 EPC/DOPA and 3:2 EPC/Chol membranes are slower than the exchange kinetics for the nAChR in EPC alone. Significantly, the slowing of peptide $^1H/^2H$ exchange in the presence of either DOPA or Chol is evident over the entire 12 h period of exposure of the nAChR membranes to ^2H_2O. The exchange profiles for the latter two membranes are similar to those observed for the nAChR in 3:1:1 EPC/DOPA/Chol. Roughly 5% more of the total number of peptide hydrogens have exchanged for the nAChR in EPC alone versus 3:2 EPC/DOPA and 3:2 EPC/Chol membranes after 2 min exposure to ^2H_2O. After 12 h, the difference in the level of peptide $^1H/^2H$ between the various membranes is closer to 10% of the total number of peptide hydrogens. The peptide hydrogens that exchange for deuterium over this 12 h time period likely correspond to those found in the extramembranous domains of the nAChR (*14*). As peptide $^1H/^2H$ exchange kinetics are strongly influenced by the amplitudes and rates of internal protein motions, the lipid-dependent changes in exchange kinetics may indicate that the internal dynamics of the entire nAChR molecule including the extramembranous domains are influenced by the presence of both DOPA and Chol in the reconstituted EPC membranes (see Discussion).

Note that the nAChR in 1:1 EPC/Chol membranes consistently exhibits more rapid exchange kinetics than the nAChR in 3:2 EPC/Chol membranes (Figure 2). The amide I band in spectra recorded from the nAChR in 1:1 EPC/Chol also exhibits a reduced intensity near 1655 cm^{-1} and an increase in intensity between 1640 and 1650 cm^{-1} relative to the nAChR in 3:2 EPC/Chol, consistent with greater exchange of α-helical peptide hydrogens. The apparent high levels (50%) of Chol in the EPC membranes reverse the general trend and may lead to an enhancement as opposed to a restriction in the rates and/or amplitudes of nAChR internal motions relative to the nAChR in 3:2 EPC/Chol membranes. An alternative possibility is that the higher levels of Chol used in the 1:1 EPC/Chol reconstitutions actually lead to the formation of Chol-rich and Chol-poor EPC vesicles and that the nAChR reconstitutes preferentially into the Chol-poor EPC membranes. The latter possibility was not examined further.

Physical Properties of the Reconstituted nAChR Membranes. A comprehensive analysis of the fluidity effects of increasing levels of both DOPA and Chol in the reconstituted EPC membranes is beyond the scope of this work. There are two regions of the FTIR spectra recorded in ^2H_2O that provide qualitative insight into the physical properties of the reconstituted membranes (Figure 4). The frequencies of the CH_2 symmetric and asymmetric stretching modes of the lipid acyl chains near 2850 and 2924 cm^{-1}, respectively, are

particularly sensitive to the phase properties of the lipid bilayer and undergo a roughly 2 cm^{-1} shift up in frequency upon transition from the gel to the liquid-crystal phase (*16*). The CH_2 stretching vibrations observed for the various nAChR membranes with increasing levels of either DOPA or Chol are all similar with symmetric and asymmetric stretching frequencies of roughly 2854 and 2924 cm^{-1}, respectively. The frequencies of these two stretching vibrations suggest that all the reconstituted membranes are found in the liquid-crystal state at room temperature, consistent with the high degree of unsaturation in each of the lipid membranes. The spectra recorded from the nAChR in 1:1 EPC/Chol membranes exhibit a slight distortion in the relative intensities of the stretching bands consistent with an unusual perturbation of lipid structure.

The carbonyl stretching vibrations of the lipid ester C═O between 1760 and 1700 cm^{-1} are also sensitive to the physical properties of the lipid membrane. Resolution enhancement shows that this band is composed of two main bands centered near 1720 and 1740 cm^{-1} which reflect hydrogen-bonded and non-hydrogen-bonded lipid ester carbonyls (*17*). The relative percentage of the lipid carbonyls found in the hydrogen- versus non-hydrogen-bonded forms is sensitive to the degree of penetration of water molecules into the headgroup region of the lipid bilayer. In a relatively ordered membrane of low fluidity, water penetration is minimal. In contrast, water penetration into an unordered membrane of relatively high fluidity is much greater, leading to a larger proportion of the lipid carbonyls in a hydrogen-bonded state.

The lipid ester carbonyl stretching vibrations observed for the nAChR reconstituted into EPC membranes with increasing levels of DOPA exhibit a striking DOPA-dependent increase in the proportion of non-hydrogen-bonded form of the lipid ester carbonyl. The increase in intensity of the non-hydrogen-bonded form suggests a tightening of the lipid−water interface and thus an ordering of the lipid membrane. The decrease in membrane fluidity suggested by the spectral changes observed in this region of the lipid membrane correlates with the decrease in peptide $^1H/^2H$ exchange kinetics. The physical properties of the DOPA-containing nAChR membranes may therefore influence the dynamic structure of the nAChR.

In contrast, the lipid ester carbonyl region does not exhibit dramatic changes indicative of an increase in membrane order with increasing Chol content. This result appears to conflict with numerous biophysical studies, including fluorescence studies of reconstituted nAChR membranes, which suggest an increased ordering effect of Chol on lipid bilayers in the liquid-crystal phase (*7*, *18*). The apparent discrepancy between these data and reports in the literature may simply reflect the formation of hydrogen bonds between Chol and the lipid ester carbonyls. The formation of hydrogen bonds between Chol and EPC likely compensates for the loss of hydrogen bonds between EPC and ^2H_2O that occurs as a result of a decrease in membrane fluidity. Based on the extensive previous work, we conclude that increasing levels of Chol also lead to a general decrease in membrane fluidity. This decrease in fluidity may result in the concomitant decrease in the internal dynamics of the nAChR as discussed above for the EPC membranes with increasing levels of DOPA.

DISCUSSION

It is increasingly recognized that internal protein dynamics play an important role in the mechanisms of protein function. A classic example is found in the binding of oxygen to myoglobin. The crystal structure of myoglobin does not exhibit a clear pathway for oxygen to travel from the aqueous environment to the heme binding site located within the interior of the protein. A static structure would require an infinite period of time for oxygen to reach its heme binding site. The ability of oxygen to bind to myoglobin on a biological time scale, however, can be rationalized by the existence of rapid small-amplitude internal motions that transiently open a "tunnel" from the exterior to the interior of the protein (*23*).

The rates at which protein peptide hydrogens exchange for those in the bulk aqueous solvent are often used as a measure of the rates and/or amplitudes of internal protein motions (*24*). While peptide hydrogens bonded directly to aqueous solvent exchange rapidly, both the formation of hydrogen bonds within protein secondary structures and the shielding of such hydrogen-bonded secondary structures from the aqueous environment in tertiary and quaternary structures dramatically slow the rates of exchange. For the exchange of hydrogen-bonded structures to occur, local motions are required to break hydrogen bonds and thus expose the peptide hydrogens to aqueous solvent. Internal motions leading to either a transient unfolding of the polypeptide backbone or the transient formation of water channels into the protein interior are also required to expose buried peptide hydrogens to the aqueous environment. The more rapid and larger the amplitudes of the internal motions, the greater exposure to the aqueous medium and thus the more rapid the exchange kinetics.

Previous studies in our laboratory have shown that upon exposure of the nAChR in 3:1:1 EPC/DOPA/Chol membranes to ^2H_2O, ~30% of the peptide hydrogens exchange for deuterium within seconds, ~50% after 30 min, ~60% after 12 h, and ~75% after prolonged exposure for several days (*14*). The nAChR in membranes composed of EPC alone undergo more rapid peptide $^1H/^2H$ exchange than the nAChR in EPC/DOPA/Chol. Increasing levels of either DOPA or Chol in EPC membranes lead to a "dose dependent" decrease in the rates of peptide $^1H/^2H$ exchange. The slowing of peptide $^1H/^2H$ exchange in the presence of either DOPA or Chol is evident within minutes as well as after hours and several days of exposure of the nAChR to ^2H_2O. The ~25% of peptide hydrogens that are normally resistant to exchange after prolonged exposure to ^2H_2O, which likely includes many of the peptide hydrogens located within the hydrophobic environment of the lipid bilayer, can be catalyzed to exchange by alkaline pH more rapidly with the nAChR in EPC versus asolectin membranes (*22*). The exchange kinetics of all the nAChR peptide hydrogens, including those found in both the intra- and extramembranous domains of the nAChR, thus appear to be influenced by lipid composition.

The lipid composition-dependent changes in peptide hydrogen exchange kinetics reflect changes in nAChR structure and/or dynamics that lead to altered hydrogen bonding and/or exposure of peptide hydrogens to the aqueous solution. We suggest that the altered exchange kinetics reflect

altered internal dynamics of the nAChR. This conclusion is based on the following observations.

(1) Only very subtle differences in the secondary structure sensitive amide I band are observed in spectra recorded from the nAChR in the different lipid membranes. These differences reflect downshifts in the frequencies of amide I component bands brought about by the altered $^1H/^2H$ exchange kinetics themselves as opposed to changes in nAChR secondary structure. Changes in nAChR secondary structure leading to altered hydrogen bonding thus are not responsible for the altered rates of peptide $^1H/^2H$ exchange.

(2) There is conflicting evidence regarding the conformations of the nAChR that are stabilized in EPC versus 3:2 EPC/DOPA and 3:2 EPC/Chol membranes. Some studies suggest that the nAChR is stabilized in a desensitized-like conformation in EPC membranes (*12*) while others suggest a resting-like conformation that is not able to undergo agonist-induced conformational change (*19*, *27*). In 3:2 EPC/DOPA and 3:2 EPC/Chol, the nAChR is capable of undergoing agonist-induced conformational change and is thus likely in a resting-like state (11). A change in conformation in EPC versus 3:2 EPC/DOPA and 3:2 EPC/Chol membranes could lead to altered exposure of peptide hydrogens that might account for the altered peptide $^1H/^2H$ exchange kinetics. Regardless of the precise conformations stabilized in the various membranes, however, the structural changes are likely subtle (*9*, *11*). In addition, agonist-induced desensitization does not lead to changes in peptide hydrogen exchange kinetics (*10*, *27*). A conformational change in EPC versus EPC/DOPA and EPC/Chol membranes that leads to altered exposure of peptide hydrogens to ^2H_2O therefore seems unlikely.

(3) It is possible that a change in the permeability of the EPC membranes occurs with either increasing DOPA or Chol, leading to changes in the exposure of transmembrane peptide hydrogens to ^2H_2O. A change in permeability, however, cannot account for the slowing of the exchange rates observed for the bulk of the peptide hydrogens (~70%; *26*) located in extramembranous domains. Note also that the difference in the total number of peptide hydrogens that have exchanged for deuterium between the nAChR in EPC versus either 3:2 EPC/DOPA or 3:2 EPC/Chol membranes increases over the time course of our exchange experiments (see Results), suggesting that the exchange kinetics of all the nAChR peptide hydrogens are affected by the changes in lipid composition.

The lipid-dependent changes in nAChR internal dynamics may correlate with changes in the fluidity of the reconstituted membranes. A decrease in fluidity with increasing levels of Chol has been documented in numerous biophysical studies (*7*, *19*). A decrease in fluidity with increasing levels of DOPA may be suggested by a decrease in the number of hydrogen-bonded lipid ester carbonyls, which may reflect a lateral tightening of the lipid bilayer and thus decreased penetration of water into the bilayer (Figure 4). Note that the increasing negative charge of the EPC/DOPA membranes could lead to a decrease in pH at the bilayer surface that may partially account for the slowing of peptide $^1H/^2H$ exchange (24). The possibility that membrane fluidity, in general, influences protein dynamics and thus protein function has been discussed (*20*), although most experiments have studied this relationship in terms of the diffusion of proteins and/or their substrates within the lipid bilayer to reach their sites of action. Further studies are currently underway in our lab to test the hypothesized link between membrane fluidity and the internal dynamics of a membrane protein. In a subsequent paper, we show that increasing levels of either DOPA or Chol both lead to an increasing ability of the nAChR to undergo Carb-induced conformational transitions (*10*). It is possible that a correlation between membrane fluidity, nAChR internal dynamics, and nAChR function may exist.

Previous studies of lipid−protein interactions, particularly with the nAChR, have examined the effects of membrane lipid composition on protein structure in an attempt to explain the well-documented effects on function. These studies have not led to detailed insight into the mechanisms of lipid−protein interactions. Our data show that membrane lipid composition can influence protein internal dynamics in the absence of detectable secondary structural change. The ability of lipids to alter internal protein dynamics could represent a previously unappreciated mechanism whereby membrane lipid composition modulates protein function.

ACKNOWLEDGMENT

We thank Joseph Von Gajasan for preparing the figures.

REFERENCES

1. Hucho, F., Tsetlin, V. I., and Machold, J. (1996) *Eur. J. Biochem. 239*, 539−557.
2. McNamee, M. G., and Fong, T. M. (1988) in *Lipid Domains and the Relationship to Membrane Function* (Aloia, R. C., Curtain, C. C., and Gordon, L. M., Eds.) pp 43−62, Alan R. Liss, Inc., New York.
3. Fong, T. M., and McNamee, M. G. (1986) *Biochemistry 25*, 830−840.
4. Fong, T. M., and McNamee, M. G. (1987) *Biochemistry 26*, 3871−3880.
5. Bhushan, A., and McNamee, M. G. (1993) *Biophys. J. 64*, 716−723.
6. Butler, D. H., and McNamee, M. G. (1993) *Biochim. Biophys. Acta 1150*, 17−24.
7. Fernandez-Ballester, G., Castresana, J., Fernandez, A. M., Arrondo, J.-L. R., Ferragut, J. A., and Gonzalez-Ros, J. M. (1994) *Biochemistry 33*, 4065−4071.
8. Sunshine, C., and McNamee, M. G. (1994) *Biochim. Biophys. Acta 1191*, 59−64.
9. Ryan, S. E., Demers, C. N., Chew, J. P., and Baenziger, J. E. (1996) *J. Biol. Chem. 271*, 24590−24597.
10. Méthot, N., Demers, C. N., and Baenziger, J. E. (1995) *Biochemistry 34*, 15142−15149.
11. Baenziger, J. E., Morris, M.-L., and Darsaut, T. E. (1999) In preparation.
12. McCarthy, M. P., and Moore, M. A. (1992) *J. Biol. Chem. 267*, 7655−7663.
13. Reid, S. E., Moffatt, D. J., and Baenziger, J. E. (1996) *Spectrochim. Acta 52*, 1347−1356.
14. Baenziger, J. E., and Méthot, N. (1995) *J. Biol. Chem. 270*, 29129−29137.
15. Méthot, N., McCarthy, M. P., and Baenziger, J. E. (1994) *Biochemistry 33*, 7709−7717.
16. Mendelsohn, R., and Mantsch, H. H. (1986) in *Progress in Protein−Lipid Interactions 2* (Watts, A., and De Pont, J. J. H. H. M., Eds.) pp 103−146, Elsevier, Amsterdam.
17. Hubner, W., and Mantsch, H. H. (1991) *Biophys. J. 59*, 1261−1272.
18. Yeagle, P. L. (1988) in *Biology of Cholesterol* (Yeagle, P. L., Ed.) pp 121−146, CRC Press, Inc., Boca Raton.
19. Rankin, S. E., Addona, G. H., Kloczewiak, M. A., Bugge, B., and Miller, K. W. (1997) *Biophys. J. 73*, 2446−2455.
20. Lenaz, G. (1987) *Biosci. Rep. 7*, 823−837.

21. Kauppinen, J. K., Moffat, D. J., Mantsch, H. H., and Cameron, D. G. (1981) *Appl. Spectrosc. 35*, 271−276.
22. Méthot, N., and Baenziger, J. E. (1998) *Biochemistry 37*, 14815−14822.
23. Karplus, M., and McCammon, J. A. (1983) *Annu. Rev. Biochem. 53*, 263−300.
24. Englander, J. J., Downer, N. W., and Teitelbaum (1972) *Annu. Rev. Biochem. 41*, 903−924.
25. McCarthy, M. P., and Stroud, R. M. (1989) *Biochemistry 28*, 40−48.
26. Unwin, N. (1993) *J. Mol. Biol. 229*, 1101−1124.
27. Raines, D. E., and Krishnan, N. S. (1998) *Biochim. Biophys. Acta 1374*, 83−93.

BI990181L